

Original Article

De novo design of a trans- β -*N*-acetylglucosaminidase activity from a GH1 β -glycosidase by mechanism engineering

Corinne André-Miral, Fankroma MT Koné², Claude Solleux, Cyrille Grandjean, Michel Dion, Vinh Tran, and Charles Tellier¹

Faculté des Sciences et des Techniques, Unité de Fonctionnalité et Ingénierie des Protéines (UFIP), Université de Nantes, UMR CNRS 6286, 2 rue de la Houssinière, BP 92208, Cedex 3 F-44322 Nantes, France

¹To whom correspondence should be addressed: Tel: +33-2-51-12-55-33; Fax: +33-2-51-12-22; e-mail: charles.tellier@univ-nantes.fr

²Present address: Université Nangui Abrogoua, 22 BP1297 Abidjan 22 (Côte d'Ivoire).

Received 24 September 2014; Revised 30 October 2014; Accepted 30 October 2014

Abstract

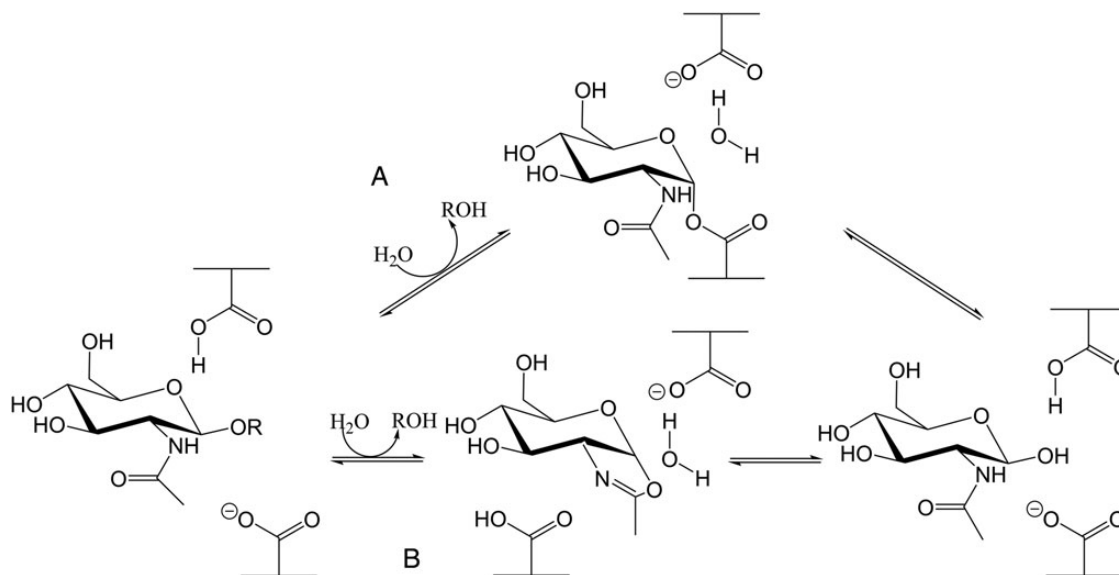
Glycoside hydrolases are particularly abundant in all areas of metabolism as they are involved in the degradation of natural polysaccharides and glycoconjugates. These enzymes are classified into 133 families (CAZy server, <http://www.cazy.org>) in which members of each family have a similar structure and catalytic mechanism. In order to understand better the structure/function relationships of these enzymes and their evolution and to develop new robust evolved glycosidases, we undertook to convert a Family 1 thermostable β -glycosidase into an *exo*- β -*N*-acetylglucosaminidase. This latter activity is totally absent in Family 1, while natural β -hexosaminidases belong to CAZy Families 3, 20 and 84. Using molecular modeling, we first showed that the docking of *N*-acetyl-D-glucosamine in the subsite –1 of the β -glycosidase from *Thermus thermophilus* (Tt β Gly) suggested several steric conflicts with active site amino-acids (N163, E338) induced by the *N*-acetyl group. Both N163A and N163D-E338G mutations induced significant *N*-acetylglucosaminidase activity in Tt β Gly. The double mutant N163D-E338G was also active on the bicyclic oxazoline substrate, suggesting that this mutated enzyme uses a catalytic mechanism involving a substrate-assisted catalysis with a noncovalent oxazoline intermediate, similar to the *N*-acetylglucosaminidases from Families 20 and 84. Furthermore, a very efficient trans-*N*-acetylglucosaminidase activity was observed when the double mutant was incubated in the presence of NAG-oxazoline as a donor and *N*-methyl-O-benzyl-N-(β -D-glucopyranosyl)-hydroxylamine as an acceptor. More generally, this work demonstrates that it is possible to exchange the specificities and catalytic mechanisms with minimal changes between phylogenetically distant protein structures.

Key words: β -glycosidase, mechanism engineering, *N*-acetylglucosaminidase, substrate-assisted catalysis, transglycosidase

Introduction

N-acetyl-hexosamines are found in many natural glycoconjugates such as in oligosaccharides present as glycoproteins or glycolipids at the cell surface (Rich and Withers 2009), in bacterial and fungal cell walls as part of the peptidoglycan (Cheng et al. 2000; Vollmer 2008)

or chitin polymers (Eijssink et al. 2010), in blood group antigens (Liu et al. 2007) and in human milk oligosaccharides (Bode and Jantscher-Krenn 2012). Protein O-GlcNAcylation is also an essential reversible post-translational modification in higher eukaryotes, which



Scheme 1. The two different catalytic mechanisms for β -*N*-acetylhexoaminidases. (A) double displacement mechanism used by GH Family 3 and (B) substrate-assisted mechanism of GH Families 20 and 84.

is involved in numerous cellular processes such as transcription, cell cycle progression and signal transduction (Hart et al. 2011). Truncated O-glycan chains that expose the terminal GlcNAc residue, identified as Tk antigen, have been identified as carcinoma-associated antigens and as potential targets for immunotherapy (Meichenin et al. 2000). As a result, the biotechnological potential of these molecules is large but currently hampered by the difficulty of their chemical synthesis. One of the enzymatic alternatives consists in using the synthetic properties of glycosidases. These usually catalyze the hydrolysis of glycoside bonds but can also synthesize glycosides, especially through the transglycosylation reaction. Some of them naturally display interesting transfer properties but yields in oligosaccharides remain generally moderate (Ogata et al. 2007; Slàmová et al. 2010).

This approach has raised more interest by the development of robust evolved glycosidases that are far more efficient than native ones. We recently applied directed evolution to the β -glycosidase of *Thermus thermophilus* (Tt β Gly; CAZy GH1 family) (Feng et al. 2005; Koné et al. 2009) and the α -L-fucosidase of *Thermotoga maritima* (GH29) (Osanzo et al. 2007). The transglycosylation activities of these glycosidases were considerably improved, with yields ranging from 60 to 80% depending on the acceptors. Due to their broad substrate specificity, the mutant transglycosidases from Tt β Gly can efficiently transfer either fucosyl, glucosyl or galactosyl units to the nonreductive end of oligosaccharides. However, Tt β Gly, like all the enzymes belonging to Family 1, does not contain β -*N*-acetylglucosaminidase activity or the corresponding transglycosylation activity, which prevents its use in the grafting of O-GlcNAc residues. Natural β -hexoaminidases belong to CAZy families GH3, GH20 and GH84, which differ in their catalytic mechanisms (Vocadlo et al. 2000; Vocadlo and Withers, 2005). β -*N*-acetylglucosaminidases from Family 3 use a catalytic mechanism similar to β -glycosidases from Family 1, which involves the formation and breakdown of a covalent α -glycosyl enzyme intermediate formed on an aspartate residue (Scheme 1A) (Slàmová et al. 2010). On the other hand, β -*N*-acetylglucosaminidases from Families 20 and 84 utilize a substrate-assisted mechanism involving the transient formation of an enzyme-sequestered oxazolinium or oxazolinium ion intermediate (Scheme 1B) (Mark et al. 2001; Macauley et al.

2005). However, both mechanisms retain the configuration at the anomeric center.

The aim of this work was to test the possibility of rationally designing an *exo*- β -*N*-acetylglucosaminidase activity from Tt β Gly glycosidase from Family 1 in order to understand how the active site residues control the mechanism and the specificity of the reaction and also possibly to use transglycosidase mutants for the synthesis of O-GlcNAc conjugates. The outcome of this work demonstrates that it is possible to evolve a β -glycosidase from Family 1 into functions that are naturally found only in Families 3 and 20, and that the choice of the mutations can dramatically affect the mechanism of hydrolysis. These results are also exploited to design new trans-*N*-acetylglucosaminidases.

Materials and methods

Strains and plasmids

Ampicillin-resistant (100 μ g/mL) *Escherichia coli* were selected on Luria-Bertani (LB) agar plates. Expression of the Tt β Gly gene was performed from the pBTac2 vector in the strain DH5 α /XL1 of *E. coli*. The expression plasmid containing the wild-type (WT) Tt β Gly gene (1.3 kb), under the control of the P_{tac} promoter and between the restriction sites EcoRI and PstI, was termed pBBGly.

Site-directed mutagenesis

β -glycosidase mutants were obtained by polymerase chain reaction (PCR) with overlapping extension. Primers D (5'-CAATTAATCATCGGCTCG) and F (5'-AATCTTCTCTCATCCGCC) flank the gene before the P_{tac} promoter and after the PstI restriction site. Twenty pmol of D or F primer was mixed with 20 pmol of mutagenic primers, 10 ng of plasmid pBBGly (with or without mutations N163A, N163D or E338G) in a 50- μ l PCR. The reaction conditions were: 1X Dynazyme buffer, 0.2 mmol/L of each dNTP and 1.5 mmol/L MgCl₂ and 2.5 U of polymerase Dynazyme Ext (Finnzymes). The sequences of mutagenic primers were the following: N163A1 (5'-TCGCCACCCTGGCCGAGCCCTGGTG) and N163A2 (5'-CACCAGGGCTCGGCCAGG

TGGCGA) for the creation of the N163A mutation. The reaction was thermocycled as follows: One cycle at 96°C, 5 min, then 30 cycles at 96°C, 30; 55°C, 30 s; 72°C, 5 min. Mutagenized PCR products were digested by the EcoRI and PstI restriction enzymes and cloned back into the pBTac2 vector digested by the same enzymes. The 1.3 kb DNA fragments encoding for mutant TtβGly enzymes were sequenced in both forward and reverse directions.

Random mutagenesis

Random mutations were introduced by error-prone PCR (EPP) (Leung et al. 1989). 20 pmol of primers D and F was mixed with 10 ng of plasmid in a 50-μL PCR. The reaction conditions were as follows: 1X Dynazyme buffer, 10 mmol dATP and dGTP, 50 mmol dTTP and dCTP, 350 μmol MgCl₂, 5 mmol MnCl₂ and 1 unit of polymerase Dynazyme Ext (Finnzymes). The reaction was thermocycled as follows: One cycle at 96°C, 5 min, then 30 cycles at 96°C, 30; 50°C, 30 s; 72°C, 2 min 30 s; 70°C, 5 min. Mutagenized PCR products were digested by EcoRI and HindIII restriction enzymes and cloned back into the pBTac2 vector. The plasmids EPP pECTorA_{N163A} and EPP pECTorA_{N163A,E338G} were used to transform *E. coli* DH5αFIQTM and express mutant in the periplasmic space using the Twin Arginine translocation (TAT) secretion system (Silvestro et al. 1989). Transformed cells (≈6000) were plated on a nitrocellulose membrane (0.45 μm, 21 × 21 cm²) lying on LB agar supplemented with 100 μg/mL ampicillin and were grown at 37°C overnight. The nitrocellulose membrane bearing ~6000 colonies was transferred onto a new LB plate containing 5-bromo-4-chloro-3-indolyl β-D-N-acetylglucosamine (X-GlcNAc, 0.5 mM) and isopropylthiogalactoside (0.05 mM) and incubated at 37°C until colored colonies appeared.

Purification of WT and mutant enzymes

Recombinant strains expressing the TtβGly mutant genes were grown in 1 L of LB medium at 37°C overnight, centrifuged and resuspended in 20 mL of lysis buffer (50 mM phosphate, 0.3 M NaCl, 10 mM imidazole, pH 8). After sonication, extracts were heated for 20 min at 70°C to precipitate most of the host proteins and centrifuged. Then the 6-His-tagged proteins were purified by immobilized ion metal-affinity chromatography: 2 L of Ni-NTA Superflow (Qiagen France, F-91974 Courtaboeuf, France) was added to the supernatant and stirred for 1 h at 4°C, then loaded onto a 10-mL column. The column was washed using 25 mL of washing buffer (50 mM phosphate, 0.3 M NaCl, 25 mM imidazole, pH 8), then 5 mL of elution buffer was added (50 mM phosphate, 0.3 M NaCl, 250 mM imidazole, pH 8). The purity of the protein (85–95%) was checked by sodium dodecyl sulfate-polyacrylamide gel electrophoresis and protein chip (Agilent).

Molecular modeling

For the enzyme, the highly resolved structure of the native TtβGly [PDB (Protein Data Bank, <http://www.rcsb.org>) code 1UG6] was used. Due to the absence of any sugar substrate in its catalytic site, the structure of the covalent intermediate between the β-glucosidase of *Bacillus polymyxa* and β-D-glucopyranosyl fluoride (PDB code 1E4I) was used as a starting template to locate any pyranose ring in the buried subsite [−1] because of the high similarity of these two enzymes at the catalytic core. This in silico replacement protocol, already described in a previous paper (Feng et al. 2005), was used here to locate NAG-thiazoline (PDB ligand code NGT), a perfect structural analog of NAG-oxazoline. As inhibitor alone, NAG-thiazoline was found

in only nine structures in complex with enzymes. Due to the very rigid bicyclic skeleton, any Cartesian coordinates can be used for in silico substrate replacement on TtβGly.

For the sake of topological comparisons between the modified catalytic context of 1UG6 (GH1) and that of other β-glucosaminidases having O-GlcNAcase activity, two structures were selected belonging to families GH84 and GH20. For GH84, only one complex with NGT ligand was solved (PDB code 2CHN) involving a bacterial enzyme (Dennis et al. 2006). Among several enzymes of the GH20 family, that of *Streptococcus gordonii* (PDB code 2EPN) was selected due to its best resolution (1.61 Å) (Langley et al. 2008).

For tridimensional (3D) structure superimpositions, the topological comparison between structures belonging to different glycoside hydrolases (GH) families is difficult when focusing on a very specific region (here, the available room delimiting the [−1] subsite). Furthermore, in the present case, although they share the same (β/α)₈ folding, they do not belong to the same clans according to CAZy classification (GH-A, GH-K and alone for GH1, GH20 and GH84, respectively). As suspected, preliminary superimpositions performed on inner β-sheets gave acceptable overall shape comparisons but incorrect 3D analyses at the subsite level. Finally, taking advantage of the inherent rigidity of the NGT inhibitor (verified in all X-ray structures where this molecule is present), the enzyme superimpositions were simply performed by pair-fitting of heavy atoms of the bicyclic structure, concerning experimental structures (2CHN, 2EPN) and a modeled one (1 double mutant of 1UG6) as well. This pair-fitting protocol is an option of the PyMOL graphic software used for molecular representation (The PyMOL Molecular Graphics System, Version 1.5.0.4 Schrödinger, LLC.).

NAG-oxazoline synthesis

A mixture of N-acetyl-D-glucosamine (1 g, 4.52 mmol), Ac₂O (9 mL) and pyridine (4.5 mL) was stirred at r.t. for 22 h. After diluting with CH₂Cl₂ (20 mL), the resulting soln. was washed successively with sat. aq. Na₂CO₃ soln. (2 × 10 mL), H₂O, H₂SO₄ (3 M soln.), H₂O, then the organic layer was dried (MgSO₄) and evaporated. Crude glucosamine peracetate was used for the following experiment without further purification. To a soln. of glucosamine peracetate (920 mg, 2.35 mmol) in 1,2-dichloroethane (30 mL), trimethylsilyl trifluoromethanesulfonate (0.5 mL, 2.76 mmol) was added dropwise, and the mixture was heated at 50° for 5 h. (CH₃)₃N (1 mL) was added and the mixture stirred for 10 min. After diluting with CH₂Cl₂ (30 mL), the mixture was washed with cold H₂O, the organic layer dried (MgSO₄) and evaporated, and the residue submitted to column chromatography (Merck silica gel 60 (0.0040–0.0063 mm), 1% Et₃N in ethyl acetate/petroleum ether 9/1) to obtain 763 mg of 2-methyl-(1,2-dideoxy-3,4,6-tri-O-acetyl-D-glucopyrano) (2,1-d)-oxazoline as a white solid (yield 75%). To a soln. of this oxazole derivative (160 mg, 0.49 mmol) in CH₃OH (5 mL) was added a solution of 5.3 M NaOCH₃ in CH₃OH (9 μL) at 0°, and the mixture was stirred for 1 h. After the reaction had finished (1 h), the solvent was evaporated (quant). The white solid obtained was dissolved in borax buffer (50 mM, pH 9.3) and stored as aliquots of 25 μL at −80°. ¹H-nuclear magnetic resonance (NMR) (D₂O, 400 MHz) δH 2.05 (d, 3H, J = 0.87 Hz, CH₃); 3.38 (ddd, 1H, J = 10.02, 4.64 and 2.86 Hz, H₅); 3.60 (dd, 1H, J = 10.02 and 6.00 Hz, H₄), 3.67 (dd, 1H, J = 12.00 and 4.64 Hz, H_{6b}); 3.81 (dd, 1H, J = 6.00 and 5.1 Hz, H₃); 3.98 (dd, 1H, J = 12.00 and 2.86 Hz, H_{6a}); 4.13 (m, 1H, H₂); 6.08 (d, 1H, J = 7.6 Hz, H₁); ¹³C-NMR (D₂O, 100 MHz) δC 14.01 (CH₃), 63.34 (C₆), 65.01 (C₅), 67.57 (C₂), 68.41 (C₃), 70.42 (C₄), 99.41 (C₁), 169.70 (CN).

Kinetic studies

All kinetic studies were performed with a (Tecan France S.A.S.U., Lyon, France) or Labsystem microplate reader at 40°C in phosphate buffer saline 1×. Initial reaction rates were calculated from the slope of the zero-order plot of product concentration (pNP) against reaction time, then the initial rates of reaction were plotted against substrate concentration and the resulting curves were fitted to the hyperbolic equation $v = V_{\max} \times [S] / (K_m + [S])$ using Origin 7.0 (OriginLab) to obtain the k_{cat} and K_m parameters. When initial rates did not exhibit saturation behavior at high substrate concentration, only k_{cat}/K_m (referred also as the *catalytic efficiency*) were determined. The k_{cat}/K_m parameter was evaluated at low substrate concentrations, when reaction rate can be approximate to the equation: $v = k_{\text{cat}}/K_M \times [E] \times [S]$. k_{cat}/K_M is then an apparent second order kinetic constant, which is determined by the initial slope of the curve $V/[E] = f([S])$.

Capillary electrophoresis measurements

Kinetics of NAG-oxazoline hydrolysis and transglycosylation activities with NAG-oxazoline as donor and *N*-methyl-*O*-benzyl-*N*-(β-D-glucopyranosyl)-hydroxylamine as acceptor were determined by capillary electrophoresis (Beckman P/ACE MDQ, Beckman Coulter, France with an uncoated fused silica capillary, 50 cm in length and 75 μm in diameter) (Teze et al. 2013). Typical experimental conditions were: 100 μL of medium containing 10 mM of 4-acetamidophenol (used as an internal standard), 30 mM NAG-oxazoline, 16 mM BnON(Me)-Glc and 100 μg of enzyme, which were incubated at 40°C in 50 mM 4-(2-hydroxyethyl)-1-piperazineethanesulfonic acid (HEPES) buffer at pH 7.8 in the capillary electrophoresis apparatus and analyzed every 20 min for 5 h. Separations were performed at 30 kV with 20 mM Borax pH 9.3 containing 50 mM sodium dodecyl sulfate as running buffer. Donors, acceptors and products were detected by ultra-violet (UV) absorbance at 200 nm and quantified by comparison with 4-acetamidophenol as internal standard.

Transglycosylation product analysis

After the enzymatic reaction had finished, the crude product was purified by reverse phase high-pressure liquid chromatography on a C18 Nucleosil VP250/10 (Macherey-Nagel, France) (300 Å, 5 μm, 10 × 250 mm) column, at a flow rate of 2.5 mL min⁻¹, with Evaporating Light Scattering Detector (Sedex 75, Sedere, France) and UV (215 nm) detection. Gradient: 0% B for 5 min, 0–80% B over 25 min or 0% B for 5 min, 0–50% B over 20 min, 50% B for 10 min, respectively. Solvent system A: H₂O; solvent system B: MeOH. Analysis of the ¹H and ¹³C-NMR resonances and subsequent structure assignments were carried out using standard 2D sequences (Correlated Spectroscopy and Heteronuclear Multiple-Quantum Correlation). The spectra were recorded with a Bruker AX400 spectrometer operating at 400 MHz for ¹H and at 100.6 MHz for ¹³C. Due to their solubility, the spectra of the saccharides were recorded in D₂O or MeOD and the chemical shifts (in ppm) were quoted from the resonance of methyl 3-(trimethylsilyl)-propansulfonate (DSS), which was used as an internal reference. Mass measurements were performed on an electrospray ionization (ESI)-Q-time-of-flight (TOF) using a quadrupole-TOF hybrid mass spectrometer (Micromass Q-TOF Ultima Global mass spectrometer, Micromass Ltd., Manchester, UK). Samples were diluted in MeOH to obtain a satisfactory intensity without signal saturation. Samples were introduced at 5 μL/min and one minute of acquisition was summed to produce the presented spectra. Nitrogen was used as sheath gas (150 L/h). The MS analyses were carried out using a typical needle voltage of 3 kV and a heated capillary

temperature of 150°C. The instrument was calibrated using MS/MS fragments of a commercial xyloglucan infused at 5 μg/mL.

After purification, the product (*N*-methyl-*O*-benzyl-*N*-(β-2-D-*N*-acetylglucopyranosyl(1→3)-β-D-glucopyranosyl)hydroxylamine) was freeze-dried and analyzed by NMR. ¹H-NMR (MeOD, 400 MHz) δH 1.92 (s, 3H, CH₃); 2.65 (s, 3H, 3H₇); 3.12–3.30 (m, 4H, H₄, H₅, H₄, H₅); 3.36–3.47 (m, 3H, H₃, H₂, H₃); 3.54–3.61 (m, 3H, H₂, 2H₆); 3.77 (dd, 1H, *J* = 12.08 and 2.16 Hz H_{6a}); 3.79 (dd, 1H, *J* = 12.04 and 1.96 Hz H_{6b}); 3.97 (d, 1H, *J* = 8.7 Hz, H₁); 4.64 (d, 1H, *J* = 8.4 Hz, H₁); 4.70 (m, 2H, 2 H₈); 7.19–7.29 (m, 5H, 5 H_{ar}). ¹³C-NMR (MeOD, 100 MHz) δC 23.16 (CH₃); 39.19 (C₇); 57.98 (C₆); 62.68 (C₆); 62.77 (C₂); 69.73 (C₅); 71.48 (C₂); 72.14 (C₅); 76.09 (C₄); 76.61 (C₈); 78.11 (C₃); 79.28 (C₄); 88.26 (C₃); 95.42 (C₁); 103.41 (C₁); 129.30, 129.48, 130.31 (5Car); 138.17 (C₉); 174.43 (CN). High resolution-ESI-MS *m/z* Calcd for C₂₂H₃₄N₂O₁₁ [M + H]⁺ 525.2060, found 525.2052.

Results

Molecular modeling of pNPGlcNAc and NAG-oxazoline in the –1 site of TtβGly

The substrate specificity of TtβGly is quite broad since this enzyme is able to hydrolyze various β-glycosides such as β-glucosides, β-fucosides and β-galactosides (Dion et al. 1999). However, it cannot hydrolyze β-*N*-acetyl-glycosides such as pNPGlcNAc. This property seems to be shared by all glycoside hydrolases of family GH1 (CAZy) (Lombard et al. 2014). Natural exo-*N*-acetylhexoaminidases are found rather in GH Families 3, 20 and 84, which have the same overall fold (β/α)₈ as the glycoside hydrolases from Family 1, but belong to different clans. The structural feature that prevents GH1 enzymes from hydrolyzing *N*-acetylglucosamine conjugates is basically the inappropriate room available in the subsite [–1] as revealed by the in silico NAG-thiazoline and β-GlcNAc replacement (docking protocol described in the “Materials and methods” section). In the first case, docking revealed a strong steric conflict with Glu338 and, to a much lesser extent, with Asn282 and Asn163 within the active site (Figure 1A). In the second case, the most severe steric conflict was due to Asn163 (Figure 1B).

The *N*-acetylhexoaminidases from Families 20 and 84 carry out hydrolysis using a substrate-assisted catalysis, which goes through a NAG-oxazolinium ion intermediate (Williams et al. 2002; Macauley et al. 2005). As a result, NAG-oxazoline is a good mimic of this intermediate. Docking the TtβGly active site with NAG-oxazoline showed that binding within the –1 site was only possible with the E338G mutant and not with the N163A mutant. On the other hand, the N163A mutation allowed β-GlcNAc docking. Such steric hindrance may explain why *N*-acetylglucosides are not substrates for this enzyme.

Furthermore, multiple sequence alignment within Family 20 and 84 hexoaminidases has revealed that the acid/base catalytic residue (E in Family 20 and D in Family 84) is always preceded in the sequence by an aspartate, which is involved in hydrogen bonding of the NAG-oxazolinium intermediate (Williams et al. 2002; Çetinbas et al. 2006). These Asp-Glu or Asp-Asp pairs provide sequence signatures of substrate-assisted catalysis within Families 20 and 84. In Family 1 glycoside hydrolases, the residue that precedes the acid–base catalytic residue is an Asn that, interestingly, corresponds to N163 in TtβGly. It was thus tempting to postulate that N163D mutation could restore an active site in the E338G mutant similar to that of GH Family 20. Topological comparisons (Figure 2) between enzymes of families GH1, GH20 and GH84 with modeled or experimentally observed

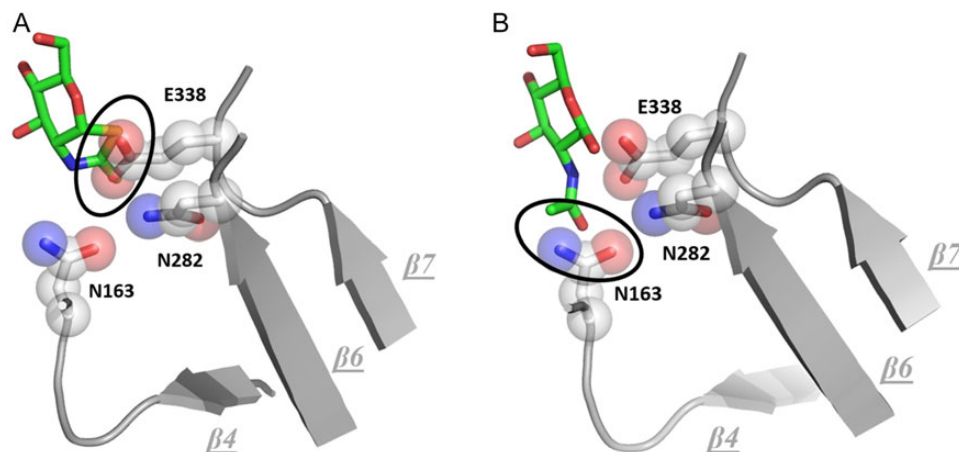


Fig. 1. *In silico* location of NAG-thiazoline (A) and β -GlcNAc (B) in the -1 subsite of Tt β Gly. Only enzyme residues (without hydrogen atoms) are shown as spheres. ‘Cartoon’ representations supporting these residues are in gray (PyMOL software). Regions of intolerable steric conflicts are circled in black.

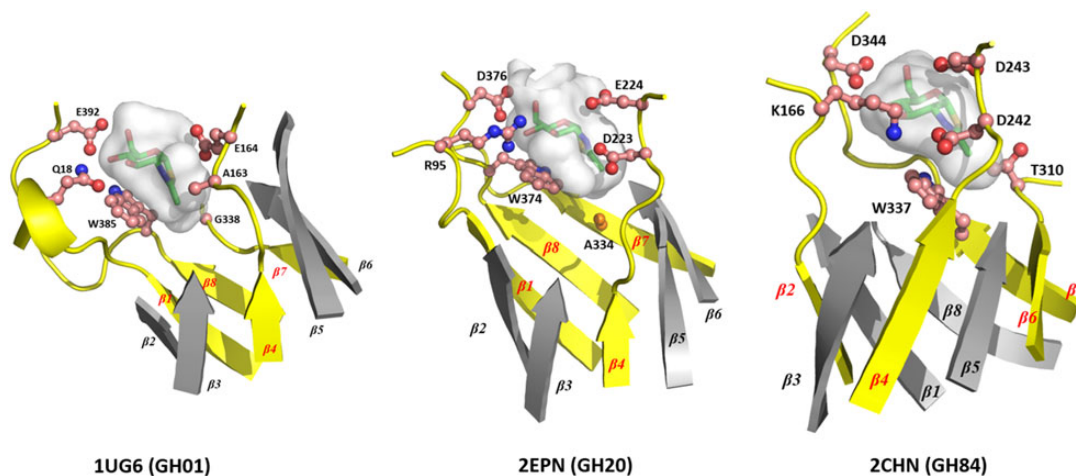


Fig. 2. Topological comparisons between modeled (1UG6 mutant) or experimental complexes (2EPN and 2CHN) involving NAG-thiazoline. White opaque surfaces represent the available room at the bottom of the catalytic site. The inhibitor (NGT) is shown as sticks. Enzyme residues stabilizing (or in contact) with the inhibitor are shown as balls and sticks. Inner beta sheets of $(\beta/\alpha)_8$ folding are shown in ‘cartoon’ representation. Those from where residues run on are colored yellow.

NAG-thiazoline (E338G mutant of 1UG6, 2EPN and 2CHN, respectively) gave relevant similarities in terms of $[-1]$ subsite cavity shapes and functionally equivalent residues, as summarized in Table I. Remarkably, these residues do not necessarily have the same topological locations, which explains why in this case, the local superimposition is much more appropriate than the overall one as would suggest any sequence alignment. For instance, E392 (1UG6), D376 (2EPN) and D344 (2CHN) (Table I) run on from beta sheets 8, 8 and 7 (for GH1, GH20 and GH84, respectively) although they are involved in substrate stabilization (hydrogen bonding of both O4 and O6 atoms of the substrate).

Analysis of the hydrolytic properties of Tt β Gly mutants

The mutations suggested by molecular modeling, N163A and N163D-E338G, were incorporated into the gene of Tt β Gly. After expression in *E. coli*, purified mutant enzymes were then tested for the hydrolysis of pNPGlcNAc and pNPGlc in 100 mM phosphate buffer pH 7.0 (Table II). While WT enzyme exhibited no detectable hydrolytic activity

Table I. 3D superimposition of functionally equivalent residues at the -1 subsite between GH1, GH20 and GH84 families

GH1 (1UG6)	GH20 (2EPN)	GH84 (2CHN)	
Q18 [β 1]	R95 [β 1]	K166 [β 2]	H bond O3
N163 [β 4]	D223 [β 4]	D242 [β 4]	Catalytic residue
D163 [β 4]			
E164 [β 4]	E224 [β 4]	D243 [β 4]	Catalytic residue
E338 [β 7]	A334 [β 7]	T310 [β 6]	Oxazoline cavity
G338 [β 7]			
W385 [β 8]	W374 [β 8]	W377 [β 7]	π stacking
E392 [β 8]	D376 [β 8]	D344 [β 7]	H bond O4 and O6

on pNPGlcNAc, both N163A and N163D-E338G mutants gave rise to a low but significant activity toward this substrate. Saturation kinetics were not observed for these mutants since substrate saturation was prevented by the low solubility of pNPGlcNAc, and only k_{cat}/K_m parameters were determined (Table II). The appearance of a β -N-

Table II. Kinetic parameters for wild-type (WT) and variant TtβGly with pNPGlc and pNPGlcNAc as substrate at 40°C, pH 6.5

Mutant	Substrate	k_{cat} (s^{-1})	K_m (mM)	k_{cat}/K_m ($mM^{-1} s^{-1}$)
WT	pNPGlucose	13.1 ± 0.5	0.11 ± 0.01	1.2×10^2
	pNPGlcNAc	nd ^a	nd	nd
N163A	pNPGlucose	2.51 ± 0.04	4.0 ± 0.2	0.62
	pNPGlcNAc	nd	nd	1.2×10^{-4}
E338G/N163A	pNPGlucose			Nd
	pNPGlcNAc			nd
E338G/N163D	pNPGlucose	$7.9 \pm 0.6 \times 10^{-3}$	15 ± 3	$\times 10^{-4}$
	pNPGlcNAc	nd	nd	1.6×10^{-4}
E338G/N163D/A211T/I216T	pNPGlucose	$9.3 \pm 0.3 \times 10^{-3}$	6.4 ± 0.7	1.4×10^{-3}
	pNPGlcNAc	$1.25 \pm 0.08 \times 10^{-2}$	25.3 ± 2.7	4.5×10^{-4}

^and, not detected.

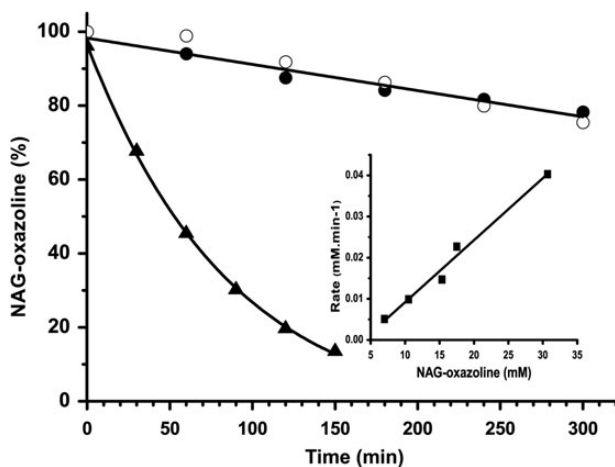


Fig. 3. Kinetics of the hydrolysis of NAG-oxazoline (50 mM). Spontaneous hydrolysis in phosphate buffer 100 mM pH 7.8 at 30°C (filled circle); With the N163A mutant (1 mg/mL) (open circle) and with the N163D-E338G mutant (1 mg/mL) (filled triangle). Inset: Initial velocities of the N163D-E338G TtβGly mutant-catalyzed hydrolysis of NAG-oxazoline. Initial velocities were corrected for the rate of the background reaction at each NAG-oxazoline concentration. The k_{cat}/K_m value, estimated from the slope, was $6.2 \pm 0.5 \times 10^{-4} \text{ mM}^{-1} \text{ s}^{-1}$.

acetylglucosaminidase activity in N163A or N163D-E338G mutants was correlated with a strong decrease in the glucosidase activity. Specificity constants k_{cat}/K_m for pNPGlucose showed a 190-fold and 2.2×10^5 -fold reduction for N163A and N163D-E338G mutants, respectively. In comparison, the double mutant N163A-E338G lost both β-glucosidase and β-*N*-acetylglucosaminidase activities.

In order to improve the β-*N*-acetylglucosaminidase activity of the N163A and N163D-E338G mutants, one cycle of directed evolution was carried out by error-prone PCR. To facilitate the screening of the *N*-acetylglucosaminidase activity directly on colonies, the mutant enzymes were expressed in the periplasmic space using the TAT secretion system. The chromogenic X-GlcNAc substrate is not internalized in the *E. coli* cytoplasm but can diffuse within the periplasm, so that hydrolysis can be detected directly on colonies if the mutant enzymes are present in this compartment. No improved enzymes were detected from a library (≈ 6000 clones) derived from the N163A mutant, and only one improved mutant was identified from the error-prone library derived from the double N163D-E338G mutant. Gene sequencing revealed that two additional mutations (A211T/I216T) were present,

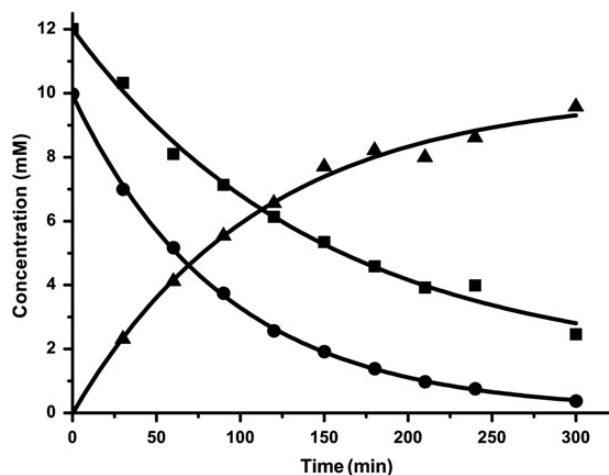


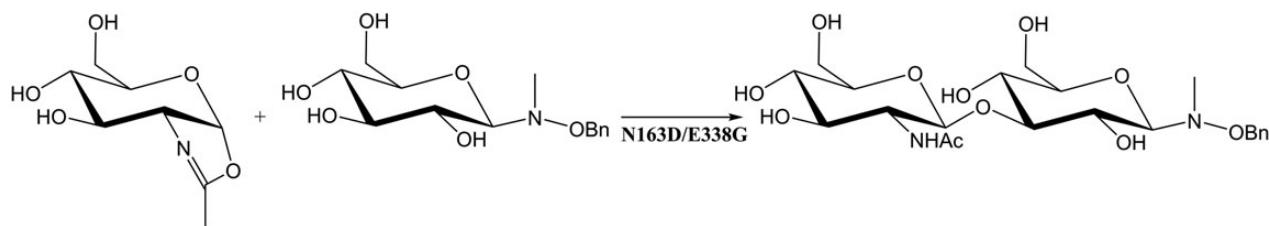
Fig. 4. Time-course of substrate consumption and product formation in the presence of N163D-E338G TtβGly mutant (10 μg) with NAG-oxazoline as donor (12 mM) and BnON(Me)-Glc (10 mM) as acceptor in 50 mM HEPES buffer, pH 7.8 at 40°C. Key: NAG-oxazoline (filled square); BnON(Me)-Glc (filled circle); BnON(Me)-GlcNAc (β1,3) Glc (filled triangle).

which slightly increased (3-fold) the k_{cat}/K_m compared with the original double mutant. However, the β-glucosidase specificity constant also increased in this evolved mutant, which resulted in a promiscuous enzyme with similar catalytic activity toward pNPGlucose and pNPGlcNAc.

NAG-oxazoline hydrolytic properties of ttβGly mutants

β-*N*-acetylglucosaminidases from Families 20 and 84 use a catalytic mechanism involving a substrate-assisted catalysis, which goes through a noncovalent bicyclic oxazoline intermediate (Scheme 1), which can be easily synthesized (Shoda et al. 2002). We anticipated that if one of the TtβGly mutants with β-*N*-acetylglucosaminidase activity uses a substrate-assisted catalytic mechanism, it could also catalyze NAG-oxazoline hydrolysis.

NAG-oxazoline is rapidly hydrolyzed to GlcNAc at acidic pH, but hydrolyzes slowly at basic pH. Kinetics of NAG-oxazoline hydrolysis were carried out at pH 7.8, where the enzyme retains most of its activity, while spontaneous hydrolysis of NAG-oxazoline is slow ($t_{1/2} = 15$ h at 30°C) (Figure 2). When the N163A mutant was added to the NAG-oxazoline solution (50 mM), no significant change in the rate of hydrolysis was observed compared with the background reaction



Scheme 2. Enzymatic transglycosylation with NAG-oxazoline as a donor.

(Figure 3). In contrast, the double mutant N163D-E338G significantly increased the rate of NAG-oxazoline hydrolysis, demonstrating that this compound is a substrate for this mutant. As no saturation was observed up to 30 mM substrate concentration, only k_{cat}/K_m was determined ($6.2 \pm 0.5 \times 10^{-4} \text{ mM}^{-1} \text{ s}^{-1}$). These results suggest that the double mutant N163D-E338G uses a mechanism involving a substrate-assisted catalysis. On the contrary, as the N163A mutant did not catalyze the hydrolysis of NAG-oxazoline and the E338 nucleophile was not mutated, this suggests that this mutant utilizes the double inversion mechanism with the formation of a covalent intermediate.

Transglycosidase activity of the N163D-E338G mutant

The ability of several transglycosylating endo-*N*-acetylglucosaminidases to catalyze the efficient transfer of sugar oxazolines to various acceptors (Ochiai et al. 2009; Rich and Withers 2009; Parsons et al. 2010) prompted us to test the transglycosylation activity of the N163D-E338G mutant. The enzymatic reaction was performed using NAG-oxazoline as a donor and *N*-methyl-*O*-benzyl-*N*-(β -D-glucopyranosyl)-hydroxylamine as an acceptor. This glucoconjugate has previously been identified as a good transglycosylation acceptor for Tt β Gly (Teze et al. 2013). A small excess of NAG-oxazoline donor (molar ratio of donor-acceptor, 1.2:1) was chosen to compensate for the hydrolysis (enzymatic and nonenzymatic) of the sugar oxazoline during the time scale of the experiment. The reaction was monitored by capillary electrophoresis until near complete consumption of substrates (Figure 4). We observed an almost complete consumption (>90%) of the acceptor to a single transglycosylation product, which was identified by NMR after purification as *N*-methyl-*O*-benzyl-*N*-(β -2-D-*N*-acetylglucopyranosyl (1 \rightarrow 3)- β -D-glucopyranosyl)hydroxylamine (Scheme 2). Such a high yield of transglycosylation was possible since no self-condensation of NAG-oxazoline was observed and no hydrolysis of the transglycosylation product was detected after long-term incubation. The excess of oxazoline was converted into GlcNAc by either spontaneous or enzymatic hydrolysis.

In contrast, a similar reaction tested with the N163A mutant gave no transglycosylation product and resulted in the complete conversion of NAG-oxazoline into GlcNAc (data not shown).

Discussion

This work shows that a rational approach based on molecular modeling was successful in broadening the substrate specificity of a Family 1 glycosidase. This is the first time that an *N*-acetylglucosaminidase activity has been created from a GH1 glycosidase. Furthermore, the results suggest that the catalytic mechanism can be controlled depending on the mutations within the active site.

Based on molecular modeling, the single N163A mutation solved part of the steric conflict between the 2-acetamido group of GlcNAc derivatives and resulted in an enzyme that showed a new hydrolytic activity on pNPGlcNAc, but not on NAG-oxazoline. Furthermore, this mutant is devoid of transglycosylation activity with NAG-oxazoline as a donor. Taken together, these results suggest that this new *N*-acetylglucosaminidase activity operates via a double displacement mechanism with a covalent glycosyl-enzyme intermediate, like *N*-acetylglucosaminidases belonging to GH3. Accordingly, additional mutation of the nucleophilic glutamate residue (E338) into a glycine resulted in a complete loss of enzymatic activity.

From this inactive double mutant (N163A-E338G), a significant *N*-acetylglucosaminidase activity was restored by replacing the N163A mutation by a N163D mutation, while this double mutant had lost the nucleophilic residue. This mutation was suggested by the sequence signature of β -*N*-acetylglucosaminidases belonging to GH20 and GH84 families, in which the two carboxylic active site residues are adjacent in the protein sequence (Asp-Glu in Family 20 and Asp-Asp in Family 84). The first Asp residue is thought to form a hydrogen bond with the nitrogen of the oxazoline ring, which stabilizes the intermediate oxazoline ring in the substrate-assisted mechanism (Scheme 1). The second carboxylate acts as a general acid-base catalytic residue. We expected that, by introducing this particular tandem Asp-Glu sequence within the active site of Tt β Gly, we could generate β -*N*-acetylglucosaminidase activity. Indeed, the N163D-E338G Tt β Gly mutant, which possesses a tandem Asp163/Glu164 pair, exhibited β -*N*-acetylglucosaminidase and trans- β -*N*-acetylglucosaminidase activities. The mechanism by which this new activity appeared is likely to be a substrate-assisted one since first, this mutant accelerated the hydrolysis of NAG-oxazoline and secondly, NAG-oxazoline is a good donor for the transglycosylation reaction.

Interestingly, the transglycosidase activity of the N163D-E338G Tt β Gly mutant was much higher than its hydrolytic activity, which resulted in a mutant enzyme that could synthesize β -GlcNAc derivatives at high yield (>90%). Until now, such a high yield of conversion from oligosaccharide-oxazoline derivatives has only been observed with *endo*- β -*N*-acetylglucosaminidases from Families 18, 56 and 85 (Shoda et al. 2002; Ochiai et al. 2009; Parsons et al. 2010). We recently demonstrated that the mutation of highly conserved residues within the -1 site of glycosidases decreases dramatically their hydrolytic activity, while their transglycosidase activity is less affected (Teze et al. 2014). The present results also confirm this observation.

Attempts to improve the β -*N*-acetylglucosaminidase activity of the Tt β Gly mutants by directed evolution resulted in a modest improvement in the hydrolytic activity of the N163D-E338G double mutant with the addition of two new mutations A211T and I216T. These mutations are not in direct contact with the active site residues, so it is difficult to explain their effect. Furthermore, these four mutations improved in a similar ratio (\approx 3-fold) the glucosidase activity and the

β -*N*-acetylglucosaminidase activity. Examples of native enzymes presenting both these activities are quite rare. To our knowledge, only the glycosidase Nag3 belonging to the family GH3 can cleave pNPGlc and pNPGlcNAc with a similar efficiency (Mayer et al. 2006). The residual glucose activity with mutants that are thought to use the substrate-assisted mechanism is surprising. One possible explanation is that the N163D mutation could replace with low efficiency the nucleophile residue absent with the E338G mutation.

Conclusion

We have demonstrated that a limited number of active site mutations within a β -glycosidase from Family 1 can change both the specificity of the enzyme and its mechanism of action so that we were able to induce a β -*N*-acetylglucosaminidase activity, which is normally found in Families 3, 20 and 84. All these glycosidase families are supported by a similar (β/α)₈ fold and these results suggest that an ancestral promiscuous enzyme with both activities could have easily evolved toward one of these activities with a few occasional mutations.

Regarding the synthetic application of these mutants, we have demonstrated that this rational approach to designing β -*N*-acetylglucosaminidases provided enzymes with high transglycosidase activity with NAG-oxazoline as donor and low hydrolytic activity, which gave a high yield of transglycosylation product. These trans- β -*N*-acetylglucosaminidases may find useful applications in the synthesis of O-GlcNAc derivatives.

Funding

This work was supported in part by the Région Pays de la Loire, France (AAP Glyconet) and F.M.T.K. from the Ivory Coast Government.

Acknowledgements

The authors are grateful to Johann Dion for the mass spectrometry measurements.

Conflict of interest

None declared.

Abbreviations

EPP, error-prone PCR; ESI, electrospray ionization; GH, glycoside hydrolases; HEPES, 4-(2-hydroxyethyl)-1-piperazineethanesulfonic acid; IPTG, isopropylthiogalactoside; LB, Luria-Bertani; NAG-oxazoline: 2-methyl-(1,2-dideoxy- α -D-glucopyranose) [2,1-d]-oxazoline; NGT: NAG-thiazoline; NMR, nuclear magnetic resonance; PCR, polymerase chain reaction; PDB, protein data bank; pNP, product concentration; TAT, Twin Arginine translocation; Tt β Gly, *Thermus thermophilus*; UV, ultra-violet; WT, wild-type; X-GlcNAc, β -D-*N*-acetylglucosamine002E; 3D, tridimensional.

References

Bode L, Jantscher-Krenn E. 2012. Structure-function relationships of human milk oligosaccharides. *Adv Nutr.* 3:383–391.
 Çetinbas N, Macauley MS, Stubbs KA, Drapala R, Vocadlo DJ. 2006. Identification of Asp174 and Asp175 as the key catalytic residues of human O-GlcNAcase by functional analysis of site-directed mutants. *Biochemistry.* 45:3835–3844.

Cheng O, Li H, Merdek K, Park JT. 2000. Molecular characterization of the *N*-acetylglucosaminidase of *Escherichia coli* and its role in cell wall recycling. *J Bacteriology.* 182:4836–4840.
 Dennis RJ, Taylor EJ, Macauley MS, Stubbs KA, Turkenburg JP, Hart SJ, Black GN, Vocadlo DJ, Davies GJ. 2006. Structure and mechanism of a bacterial β -glucosaminidase having O-GlcNAcase activity. *Nat Struct Mol Biol.* 13:365–371.
 Dion M, Fourage L, Hallet JN, Colas B. 1999. Cloning and expression of a beta-glycosidase gene from *Thermus thermophilus*. Sequence and biochemical characterization of the encoded enzyme. *Glycoconj J.* 16:27–37.
 Eijsink V, Hoell I, Vaaje-Kolstada G. 2010. Structure and function of enzymes acting on chitin and chitosan. *Biotechnol Genet Eng Rev.* 27:331–366.
 Feng HY, Drone J, Hoffmann L, Tran V, Tellier C, Rabiller C, Dion M. 2005. Converting a β -glycosidase into a β -transglycosidase by directed evolution. *J Biol Chem.* 280:37088–37097.
 Hart GW, Slawson C, Ramirez-Correa G, Lagerlof O. 2011. Cross talk between O-GlcNAcylation and phosphorylation: Roles in signaling, transcription, and chronic disease. *Annu Rev Biochem.* 80:825–858.
 Koné FM, Le Béchech M, Sine JP, Dion M, Tellier C. 2009. Digital screening methodology for the directed evolution of transglycosidases. *Protein Eng Des Sel.* 22:37–44.
 Langley DB, Harty DW, Jacques NA, Hunter N, Guss JM, Collyer CA. 2008. Structure of *N*-acetyl-beta-D-glucosaminidase (GcnA) from the endocarditis pathogen *Streptococcus gordonii* and its complex with the mechanism-based inhibitor NAG-thiazoline. *J Mol Biol.* 377:104–116.
 Leung DW, Chen E, Goeddel DV. 1989. A method for random mutagenesis of a defined DNA segment using a modified polymerase chain reaction. *Technique.* 1:11–15.
 Liu QP, Sulzenbacher G, Yuan H, Bennett EP, Pietz G, Saunders K, Spence J, Nudelman E, Levery SB, White T, et al. 2007. Bacterial glycosidases for the production of universal red blood cells. *Nat Biotechnol.* 25:454–464.
 Lombard V, Golaconda Ramulu H, Drula E, Coutinho PM, Henrissat B. 2014. The carbohydrate-active enzymes database (CAZy) in 2013. *Nucleic Acids Res.* 42:D490–D495.
 Macauley MS, Whitworth GE, Debowski AW, Chin D, Vocadlo DJ. 2005. O-GlcNAcase uses substrate-assisted catalysis. *J Biol Chem.* 280:25313–25322.
 Mark BL, Vocadlo DJ, Knapp S, Triggs-Raine BL, Withers SG, James MN. 2001. Crystallographic evidence for substrate-assisted catalysis in a bacterial beta-hexosaminidase. *J Biol Chem.* 276:10330–10337.
 Mayer C, Vocadlo DJ, Mah M, Rupitz K, Stoll D, Warren RA, Withers SG. 2006. Characterization of a beta-*N*-acetylhexosaminidase and a beta-*N*-acetylglucosaminidase/beta-glucosidase from *Cellulomonas fimi*. *FEBS J.* 273:2929–2941.
 Meichenin M, Rocher J, Galanina O, Bovin N, Nifant'ev N, Sherman A, Cassagnau E, Heymann MF, Fraser RH, Le Pendu J. 2000. Tk, a new colon tumor-associated antigen resulting from altered O-glycosylation. *Cancer Res.* 60:5499–5507.
 Ochiai H, Huang W, Wang LX. 2009. Endo- β -*N*-acetylglucosaminidase-catalysed polymerization of β -GlcP-(1 \rightarrow 4)-GlcPNAc oxazoline: A revisit to enzymatic transglycosylation. *Carbohydr Res.* 344:592–598.
 Ogata M, Zeng X, Usui T, Uzawa H. 2007. Substrate specificity of *N*-acetylhexosaminidase from *Aspergillus oryzae* to artificial glycosyl acceptors having various substituents at the reducing ends. *Carbohydr Res.* 342:23–30.
 Osanjo G, Dion M, Drone J, Solleux C, Tran V, Rabiller C, Tellier C. 2007. Directed evolution of the α -L-fucosidase from *Thermotoga maritima* into an α -L-transfucosidase. *Biochemistry.* 46:1022–1033.
 Parsons TB, Patel MK, Boraston AB, Vocadlo DJ, Fairbanks AJ. 2010. *Streptococcus pneumoniae* endohexosaminidase D. feasibility of using N-glycan oxazoline donors for synthetic glycosylation of a GlcNAc-asparagine acceptor. *Org Biomol Chem.* 8:1861–1869.
 Rich JR, Withers SG. 2009. Emerging methods for the production of homogeneous human glycoproteins. *Nat Chem Biol.* 5:206–215.
 Shoda SI, Fujita M, Lohavisavapanichi C, Misawa Y, Ushizaki K, Tawata Y, Kuriyama M, Kohri M, Kuwata H. 2002. Efficient method for the

- elongation of the N-acetylglucosamine unit by combined use of chitinase and β -galactosidase. *Helv Chim Acta*. 85:3919–3936.
- Silvestro A, Pommier J, Pascal MC, Giordano G. 1989. The inducible trimethylamine N-oxide reductase of *Escherichia coli* K12: Its localization and inducers. *Biochim Biophys Acta*. 999:208–216.
- Slámová K, Bojarova P, Petraskova L, Kren V. 2010. β -N-acetylhexosaminidase: What's in a name?. *Biotechnology Adv*. 28:682–693.
- Teze D, Dion M, Daligault F, Tran V, André-Miral C, Tellier C. 2013. Alkoxyamino glycoside acceptors for the regioselective synthesis of oligosaccharides using glycosynthases and transglycosidases. *Bioorg Med Chem Lett*. 23:448–451.
- Teze D, Hendrickx J, Czjzek M, Ropartz D, Sanejouand YH, Tran V, Tellier C, Dion M. 2014. Semi-rational approach for converting a GH1 β -glycosidase into a β -transglycosidase. *Protein Eng Des Sel*. 27:13–19.
- Vocadlo DJ, Mayer C, Shouming H, Withers SG. 2000. Mechanism of action and identification of Asp242 as the catalytic nucleophile of *Vibrio furnisii* N-acetyl- β -D-glucosaminidase using 2-acetamido-2-deoxy-5-fluoro- α -L-idopyranosyl fluoride. *Biochemistry*. 39:117–126.
- Vocadlo DJ, Withers SG. 2005. Detailed comparative analysis of the catalytic mechanism of β -N-acetylglucosaminidases from families 3 and 20 of glycoside hydrolases. *Biochemistry*. 44:12809–12818.
- Vollmer W. 2008. Structural variation in the glycan strands of bacterial peptidoglycan. *FEMS Microbiol Rev*. 32:287–306.
- Williams SJ, Mark BL, Vocadlo DJ, James MN, Withers SG. 2002. Aspartate 313 in the *Streptomyces plicatus* hexosaminidase plays a critical role in substrate-assisted catalysis by orienting the 2-acetamido group and stabilizing the transition state. *J Biol Chem*. 277:40055–40065.